PCCP

Packing states of multilamellar vesicles in a nonionic surfactant system

T. D. Le,*[a] U. Olsson[a] and K. Mortensen[b]

[a] *Center for Chemistry and Chemical Engineering, Division of Physical Chemistry 1, Lund University, PO Box 124, S-22100 Lund, Sweden. E-mail: Thao.Le@fkem1.lu.se*
[b] *Risø National Laboratory, Department of Condensed Matter Physics and Chemistry, PO Box 49, DK-4000 Roskilde, Denmark*

Received 17th August 2000, Accepted 10th January 2001
First published as an Advance Article on the web 13th March 2001

Lyotropic lamellar phases under shear flow have been shown to form multilamellar vesicles (MLVs), an onion-like structure. The size of the vesicles is governed by the shear imposed on the sample. Previously, we studied the structural transformation from multilamellar vesicles to lamellae to sponge under shear. Here, we focused only in the MLV region, L_α^*, of a temperature sensitive surfactant system ($C_{12}E_4$–water) to investigate the packing of multilamellar vesicles as a function of temperature under constant shear. Two sets of temperature scan experiments were performed in the L_α^* phase using the noninvasive small-angle neutron scattering (SANS) technique, one while heating and the other while cooling the sample. Data from the heating and cooling cycles were used to demonstrate reversibility of the system. Three states of packing can be identified from the scattering profiles: isotropic at low (**i**) and high (**iii**) temperature ranges, and hexagonal with six spots at an intermediate temperature interval (**ii**). The hexagonal 2-D SANS patterns reveal different peak intensities under shear, which upon cessation of shear relaxes to a symmetrical scattering pattern. The hexagonal scattering pattern from state **ii** is a layering effect of vesicles into a honeycomb type structure (spherulites).

Introduction

There are several methods for encapsulating materials for pharmaceutical or industrial applications. Two of the most frequently used are liposomes (made of lipids) and nanospheres (made of polymers). In recent years, studies on lyotropic lamellar phases under shear have introduced another means of encapsulation called spherulites (made of surfactants and, in some rare cases, polymers).

Spherulites are closely packed vesicles made of repeated lamellar units forming onion-like structures whose size is governed by shear and can vary between 0.1 and 50 μm and have between 10 to 1000 layers. The multilamellar vesicles, MLVs, made in this way have similar properties as the lamellar phase, *e.g.*, solubilization of water or oil, interlamellar spacing, and bending rigidity. In recent years, a number of studies have explored the prospects of encapsulating submicron particles,[1] fatty acids, enzymes[2] and the use of MLVs as chemical microreactors[3] and as a pH regulator inside the microcapsules[4] using the so-called spherulite technology, which originated from research studies on lamellar phases under shear. At rest, the lamellar state is the equilibrium structure. When subjected to shear, however, the phase experiences a series of transformations that modify the topology of the lamellae in space relative to the direction of shear field.[5,6]

Conventional methods for producing a phase equilibrium diagram are made either by shaking, stirring, vortexing, or centrifuging a sample to accelerate the mixing process. Depending on the sample concentration, a gentle shake can induce a new structure or perturb the state of a phase. Shear experiments on lamellar phases have used this fact to induce a transition from lamellar to multilamellar vesicle phase under a controlled environment; in which case, it was found that monodisperse multilamellar vesicles can be produced.[7]

Some experimental cases have shown that under certain conditions the dispersion of multilamellar vesicles can undergo a transition into an ordered state under shear. This state can be kept for weeks to months at rest, depending on the system. When, however, dispersed in excess solvent (*e.g.*, water), the spherulites are exposed to an osmotic gradient, which can drastically turn a metastable state into an unstable state. The rheology in this region, while fascinating, is complicated by a number of experimental factors. To understand the underlying phenomenon, experiments must be extended to include the coupling between intensive parameters such as charge, temperature, concentration, and flow effect which help in stabilizing the multilamellar structure. The orientation diagram,[5] where a connection is made between shear and structure under flow, and temperature–composition structural diagram at constant shear rate[6] have provided valuable insights into the mechanical response of surfactant membranes under shear flow.

It is not yet understood why multilamellar vesicles are often formed when exposing a lamellar phase to shear. The relative stability of different surfactant aggregate structures is often analyzed in terms of Helfrich curvature energy. To leading order in the curvatures, the local curvature free energy density can be written as

$$g_c = 2\kappa(H - H_0) + \bar{\kappa}K. \quad (1)$$

Here, H and K are the mean and Gaussian curvatures, κ and $\bar{\kappa}$ are the bending and saddle-splay moduli, respectively, and H_0 is the spontaneous curvature of the monolayer. The curvature energy of a given surfactant film configuration is then

 DOI: 10.1039/b006747o

given by integrating eqn. (1) over the surface. A symmetric surfactant bilayer has zero spontaneous curvature and the curvature free energy per unit area can be written as

$$G_c/A = 2\kappa_b\langle H_b^2\rangle + \bar{\kappa}_b\langle K_b\rangle, \quad (2)$$

where the angular brackets denote surface averages and we have used subscript b to denote that we are working with bilayer properties evaluated at the bilayer midplane. From eqn. (2) we see that forming a vesicle from the reference planar lamellar state has the cost

$$G_c^{ves} = 4\pi(2\kappa_b + \bar{\kappa}_b). \quad (3)$$

With this type of reasoning, spontaneous vesiculation is predicted when $\bar{\kappa}_b < -2\kappa_b$.

The parameter $\bar{\kappa}_b$ can take positive or negative values and can be viewed as a tuning parameter for the bilayer topology. When positive, it stabilizes a multiply connected membrane as in the L_3 (sponge) phase and, as seen above, it can stabilize vesicles when being smaller than $-2\kappa_b$. At intermediate values the planar lamellar state is stable. For nonionic surfactants of the ethylene oxide type, the tuning of $\bar{\kappa}_b$ can be achieved by varying the temperature. In fact, we observed recently,[6] in a related nonionic system, the successive sequence: MLV–planar lamellae–sponge structure, as a function of increasing temperature in a continuous shear experiment.

The temperature dependence of the nonionic systems is commonly described in terms of the temperature dependence of the monolayer spontaneous curvature, H_0, which decreases with increasing temperature. The bilayer $\bar{\kappa}_b$ is related to the bending properties of the monolayer evaluated at the polar/apolar interface, a distance l from the bilayer midplane, as

$$\bar{\kappa}_b = 2\bar{\kappa} - 4\kappa l H_0, \quad (4)$$

where κ and $\bar{\kappa}$ are the monolayer bending and saddle splay moduli, respectively. From eqn. (4) we see that a decrease in H_0 corresponds to an increase in $\bar{\kappa}_b$. With eqn. (2), we can reformulate the stability requirement for vesicles $\bar{\kappa}_b < -2\kappa_b$ in terms of monolayers properties as:

$$2\bar{\kappa} - 4\kappa l H_0 < -4\kappa, \quad (5)$$

in which we have introduced $\kappa_b = 2\kappa$. Eqn. (5) can be rearranged to obtain

$$H_0 > \frac{1}{l}\left(1 + \frac{\bar{\kappa}}{2\kappa}\right). \quad (6)$$

However, when $H_0 = (1 + \bar{\kappa}/2\kappa)/l$ the curvature energy is minimized by spherical micelles of radius l (*cf.* ref. 8), and one rather expects a micellar (L_1) phase instead under these conditions. With this reasoning, we see that when shear induced vesicles or MLV structures are observed in the lamellar phase $\bar{\kappa}_b$ is still significantly larger than -2κ. Nevertheless, $\bar{\kappa}_b$ plays a role because the stability of the MLVs under shear is temperature dependent.

In the present study, we used a two component system, surfactant and water. The surfactant is nonionic of the type C_nE_m, and we have chosen one where the hydrophobic tail n and the hydrophilic head group m are 12 and 4 ($C_{12}E_4$), respectively. The phase equilibria of $C_{12}E_4$–water is known[9,10] and shows a broad lamellar phase that spans *ca.* 40 °C in temperature and surfactant concentration up to 85% w/w. There has been a few related studies[6,11,12] examining the effect of shear on the lamellar phase, thus providing a suitable complement to the present investigation. Here, we focus primarily on the topological transformation from lamellar to multilamellar vesicles to examine the packing of multilamellar vesicles in the MLV region. With the use of a temperature sensitive system, we can conveniently access the different packing states and the mechanical threshold of the system at a fixed shear rate.

Experimental

Materials and sample preparation

The bilayer membrane system used in this study was made of tetra(ethylene glycol) mono-*n*-decyl ether, abbreviated as $C_{12}E_4$ (Nikko Chemicals Co., Tokyo) and D_2O (Dr. Glaser AG, Basel). The deuterium oxide (D_2O) was used to enhance the contrast between the membrane structure and solvent for neutron scattering experiments. Both surfactant and solvent have purity better than 99.8% and were used without further purification. All samples were prepared by weight, and the volume fraction of surfactant Φ was calculated using the following densities: 0.95 g cm^{-3} ($C_{12}E_4$) and 1.11 g cm^{-3} (D_2O).

In this binary system, an isotropic sponge (L_3) phase exists at high temperatures and a lamellar phase at low temperatures.[9,10] Within a given temperature interval, a gentle shake can transform lamellae into multilamellar vesicles, resulting in a drastic increase in viscosity. This shear thickening behavior poses a problem in concentrated samples since it can lead to inadequate mixing of the solution. To circumvent this problem, each sample was prepared by placing the sample tube into a thermostatic bath, the bath temperature raised until the L_3 phase is reached (isotropically clear solution with low viscosity), the sample mixed and allowed to gradually cool to the L_α phase (at *ca.* 25 °C).

Shear experiments using small-angle neutron scattering (SANS)

The small-angle neutron scattering (SANS) experiments were performed at Risø National Laboratory, Denmark. Two neutron wavelengths (λ = 3.8 and 5.7 Å) and three sample-to-detector distances (2, 3 and 6 m) were used to cover a range of scattering vector q, $|\vec{q}| = 4\pi \sin(\theta/2)/\lambda$, between 0.002 and 0.2 Å^{-1}. The resolution of the wavelength, $\Delta\lambda/\lambda$, was 18%. The scattered intensity was recorded by a two-dimensional position sensitive area (128 pixel × 128 pixel) detector. The temperature of the sample was controlled within ±0.2 °C by an external thermostatic water bath.

Measurements were made in the through-view configuration, *i.e.*, the incident beam was parallel to the velocity gradient direction (y-axis) and the scattered intensity was monitored in the x–z plane (x is the flow direction and z is the neutral direction). The shear rate was calculated[13] using $\dot{\gamma} = 2\pi\Omega\langle R\rangle/(R_o - R_i)$, where Ω is the rotation speed, R_i = 14.5 mm and R_o = 15 mm are the inner and outer radii, and $\langle R\rangle = (R_o + R_i)/2$. The shear cell used was a Couette type with two concentric cylinders, where the outer is the stator and the inner is the rotor. The circular neutron beam with a diameter of 5 mm was passed radially through the center of the cylinders yielding a total neutron path length 2 times the annular gap. The sample size was *ca.* 1.5 ml. The design and performance of the Couette cell are described in detail in ref. 14.

Using the *in-situ* SANS technique, we probed the structures and state of arrangements under shear of the shear-induced multilamellar vesicle phase. To reduce the number of variables in the study, the shear rate was fixed at $\dot{\gamma} = 100 \pm 5$ s^{-1} and measurements were made while heating the sample. Measurements were also made while cooling the sample to demonstrate reversibility. The scan time varied from sample to sample due to the experimental conditions, *e.g.*, surfactant concentration, sample-to-detector distance, and wavelength of the neutron. In general, the scan time increases with dilution, *e.g.* 600 s per scan for the surfactant volume fraction $\Phi = 0.06$ sample, but only 180 s per scan for $\Phi = 0.44$.

Results and discussion

Temperature scan experiments

The advantage of using a temperature sensative system is that structural change can conveniently be monitored by varying the temperature. Here, we fixed the shear rate at $\dot{\gamma} = 100\ s^{-1}$ and performed SANS measurements while gradually heating (or cooling) the sample. As indicated in the Experimental section, the acquisition time was chosen in the range between 180 and 600 s, which translates to a range of 18 000–60 000 strain units for concentrated and dilute samples, respectively, per recorded scattering pattern. The procedures above were carried out for four different volume fractions of $C_{12}E_4$ in the range $0.06 < \Phi < 0.44$, from which we obtained a data set comprising of a few hundred 2-D spectra that could be used to construct a temperature *vs.* concentration structural diagram at constant shear rate.

The present system exhibits similar behavior under shear as another nonionic system, $C_{10}E_3$–water.[6] At the temperature range from 25 to 38–50 °C, depending on the concentration, the steady state structure under shear flow is the multilamellar vesicles, and we refer to this region as L_α^*. From this structure, we obtain an isotropic scattering (except at higher concentrations as we will demonstrate below) which, in principle, is also consistent with a powder lamellar phase. The presence of MLVs, however, has been proven previously by small angle light scattering.[12] At higher temperatures, the structure transforms into a planar lamellar (L_α) state. Note that the present study used only the radial beam configuration. In a previous study[6] where we have measurements covering the radial (q_x–q_z) and tangential (q_y–q_z) scattering planes, we concluded that the preferred lamellar orientation was with the bilayer normal in the gradient direction (*i.e.*, the bilayers are parallel with the flow). However, a minor population remains with the bilayer normal pointing perpendicularly to the flow direction, giving rise to the scattering in the neutral direction. As found in that system,[6] the crossover from L_α^* to L_α involves a coexistence of the two structures and we denote this coexistence region $L_\alpha^* + L_\alpha$. The obtained temperature *vs.* concentration structural diagram is presented in Fig. 1. At much higher temperatures we also observed the L_3 (sponge) phase, but this region was not investigated in detail here.

As noted earlier, the primary focus of the present study is on the shear-induced multilamellar vesicles in the L_α^* region and the different packing states. Fig. 2 shows representative SANS data collected during a temperature scan experiment of a $\Phi = 0.44$ sample. On the left hand side are 2-D SANS spectra obtained at different temperature intervals, and on the right are the corresponding azimuthal traces (circular averaged intensity within $0.08 < q < 0.12$). Fig. 2 shows three distinctly different scattering patterns obtained inside the L_α^* region, labeled as states **i**, **ii** and **iii**. States **i** and **iii** are present throughout the concentration range investigated. Due to the limit of the structure factor peak, state **ii** could only be detected at concentration above $\Phi > 0.2$. The temperature intervals where these states were observed are marked as (a)–(e) in Fig. 1.

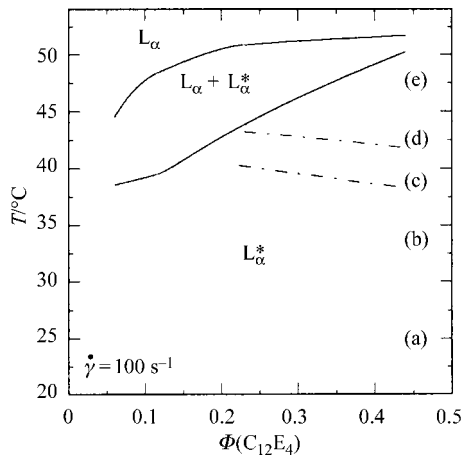

Fig. 1 Temperature–composition diagram of the $C_{12}E_4$–D_2O system under Couette flow ($\dot{\gamma} = 100\ s^{-1}$). From low to high temperatures: multilamellar vesicle phase (L_α^*), and planar lamellar phase (L_α). The L_α^* phase is the main focus of the present study. (a)–(e) are the corresponding temperatures of SANS data shown in Fig. 2.

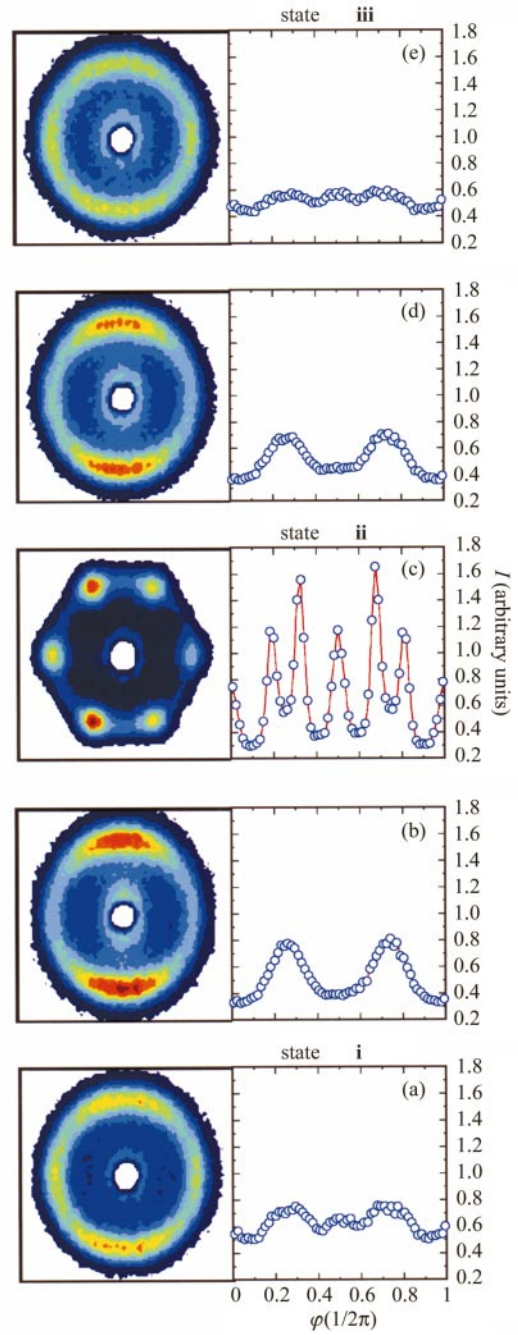

Fig. 2 Representative SANS data collected during a temperature scan experiment. The example shown is for a $\Phi = 0.44$ sample recorded while heating at a rate of 1 °C per 12.9 min and shearing at a rate of 100 s^{-1}. Shown on the left are 2-D SANS spectra and on the right are the corresponding azimuthal traces averaged around a q-band 0.08–0.12 $Å^{-1}$: (a) 25.0, (b) 33.7, (c) 38.9, (d) 42.6 and (e) 47.5 °C. The contours correspond to a linear scale, and the maximum q-value is 0.2 $Å^{-1}$.

Temperature dependence of multilamellar vesicles

The general features of the scattering in state **i** (low temperature range) and state **iii** (high temperature range) are

similar in that the scattering is almost isotropic in the (q_x, q_z) plane of the 2-D SANS spectra and by the azimuthal traces around a q-band.[15] These scattering profiles are indicative of scattering behavior for a multilamellar vesicles phase, as was found in a related system[6] where small-angle neutron (radial and tangential beam configurations) and depolarized light scattering were used to demonstrate the existence of shear-induced mutilamellar vesicles at temperatures below the planar lamellar phase.

A more detailed analysis of the scattered intensity in states **i** and **iii** reveals minor differences between the two states. Fig. 3(a) and (b) are I *vs.* q plots comparing the scattering curves in the neutral (q_z) and flow (q_x) directions. The position of the Bragg peak is the same in states **i** and **iii**. The larger intensity difference in the $(q_x - q_z)$ plane in Fig. 3(a) indicates elongation (*ca.* 10%) in the flow field and that the multilamellar vesicles at lower temperature (state **i**) are more susceptible to flow than the more organized structure in state **iii**.

The scattering profiles in regions **i** + **ii** and **ii** + **iii**, as shown in Fig. 2(b) and (d), are intermediates between the different states. In these intermediate states, the bilayers reorganize and redistribute themselves to form the hexagonal pattern in state **ii**. The asymetrical hexagonal pattern will be discussed in a latter section. Fig. 4 shows a detailed intensity analysis comparing the scattering curves in the flow (left) and neutral (right) directions obtained from states **i** (bottom) and **iii** (top) and the corresponding intermediates. The plots reveal substantial intensity difference in both the flow and neutral directions for the intermediates. These intensity curves qualitatively show the gradual transitions between the different states. The scattered intensities from states **i** and **iii**, as shown in Fig. 3, are virtually isotropic in the (q_x, q_z) plane.

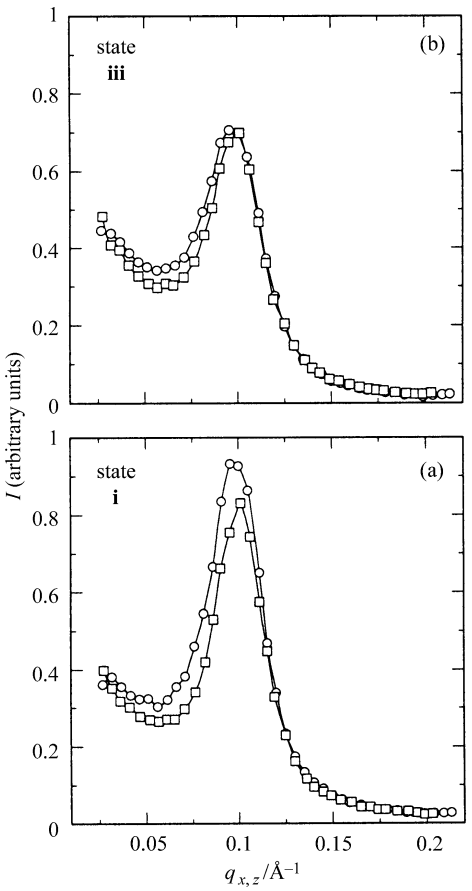

Fig. 3 A comparison between states **i** and **iii**. Shown are the $I(q_x)$, (□) and $I(q_z)$, (○), for states **i** and **iii** measured at (a) 25.0 and (b) 47.5 °C, respectively. Note that the scattered intensity profiles in state **i** are higher and less symmetric than the ones in state **iii**. Similar observation can be seen from the azimuthal traces, Fig. 2(a) and (e).

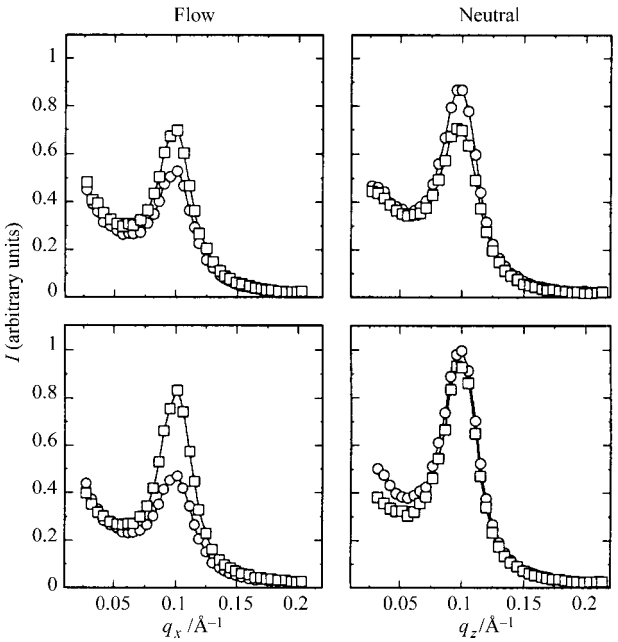

Fig. 4 Comparative analysis of the scattered intensity in the (q_x, q_z) plane obtained from states **i** and **iii** and from intermediates adjacent to these states. Shown are: (bottom) state **i** (○) and intermediate (□) and (top) state **iii** (○) and intermediate (□). The corresponding 2-D SANS spectra, azimuthal traces, and temperatures are shown in Fig. 2.

Structural properties of mutilamellar vesicles

From the Bragg peak position in Fig. 3(b), we obtain $d_{MLV} = 6.58$ nm. If we assume that the first shell of a multilamellar vesicle has a thickness d_{MLV}, the spacing between layers, and that d_{MLV} is uniform throughout the MLV structure, the radius of the MLV, R_{MLV}, can then be written as

$$R_{MLV} = n_{sh}\, d_{MLV}. \tag{7}$$

Diat *et al.*[5,11] have shown a dependence of the MLV size on the shear rate through a simple force balance between the elastic force stored in a spherical vesicle

$$F_e = 4\pi(2\kappa_b + \bar{\kappa}_b)/d \tag{8}$$

and the viscous force experienced by an object under flow

$$F_v = \eta\dot{\gamma}R_{MLV}^2, \tag{9}$$

where η is the mean viscosity representing the viscous force on a vesicle in the presence of its neighbors. The combined eqns. (8) and (9) suggests that the size of the MLVs is proportional to shear rate to the power $-1/2$. We should point out that while the exact nature of parameter(s) controlling the size of the multilamellar vesicles is still under debate,[16–18] a number of studies have suggested that the size is related to the shear rate as $R_{MLV} \propto \dot{\gamma}^{-1/2}$. A recent study by Müller *et al.*[12] performed on a 40 wt.% concentration of the same system as the present is one such example. The techniques used were small-angle light scattering and nuclear magnetic resonance (NMR) and measurements were made at 25 °C shearing between 10 to 70 s^{-1}. These experimental conditions are compatible with the present study, thus can be used to estimate some structural properties such as the size of the MLVs and the number of shells.

From Müller *et al.*'s plot of q_{max} *vs.* $\dot{\gamma}^{-1/2}$, an extrapolation to $\dot{\gamma} = 100$ s^{-1} yields $R_{MLV} = 0.45$ μm. Solving eqn. (7) for n_{sh} yields a value of 68 for the number of shells. The estimate given here is for a $\Phi = 0.44$ sample shearing at a rate of 100 s^{-1} at 25 °C. The above values can also be used to get an estimate for the bending properties of the bilayers, *e.g.*, κ_b and $\bar{\kappa}_b$. From rheology, the viscosity has been determined to be $\eta = 1.5$ Pa s and substituting this and the above values into

eqns. (8) and (9) and solving for $(2\kappa_b + \bar{\kappa}_b)$ leads to a value of $3.9kT$, which is consistent with the magnitude of the values found for a number of surfactant systems.[7]

The curvature energy for forming a vesicle is $G_c(T) = 4\pi[2\kappa_b + \bar{\kappa}_b(T)]$, which relies on the interplay between the bending and saddle-splay moduli. From above, a value of $3.9kT$ was found for the term in brackets. The value of κ_b can be measured by scattering techniques[19] or NMR.[20] The parameter $\bar{\kappa}_b$, on the other hand, is more difficult to determine due to the accessibility of $\bar{\kappa}$ monolayer by experiments. The importance of this analysis is not in the actual values of these parameters, but rather to illustrate the delicate balance between these phenomenological parameters that transforms from planar bilayers to spherical vesicles.[6] In the present case, temperature was used to vary the saddle-splay modulus $\bar{\kappa}_b$, and in the L_α^* region the value of $\bar{\kappa}_b$ becomes less negative with increasing temperature.

Shear-induced layering in the L_α^* phase

The temperature scan sequence shown in Fig. 2 reveals isotropic scattering at low temperature (state **i**) and hexagonal ordering (state **ii**) and back to isotropic scattering at high temperature (state **iii**). The isotropic scattering profiles in the L_α^* region of nonionic surfactant systems have been demonstrated to correspond to multilamellar vesicles in a few nonionic systems.[6,12] The asymmetrical scattering profiles between these states are indicative of intermediates, where the bilayers rearrange to form state **ii**.

As shown in Fig. 5, the intensity peaks are more pronounced in $\Phi = 0.44$, Fig. 5(b), than 0.23, Fig. 5(a), and vanishes below this concentration. In principle, this can be due to an increasing size polydispersity with increasing dilution. However, in the monodisperse case, this is still the expected trend as the interbilayer spacing increases. At $\Phi = 0.44$, the hydrated bilayers are nearly close packed. The anisotropy (hexagonal structure), caused by the interactions between the close packed MLVs, then propagates far into the inner layers. At $\Phi = 0.2$, the spacing is larger and the anisotropy does not propagate as far. A schematic drawing is shown in Fig. 6, where the shells of MLVs at sufficiently high dilution are expected to be less uniformly arranged due to having more room available for movement of the bilayers as the water layers increase with dilution. As the bilayers become unevenly distributed, the intensity decreases and vanishes at very high dilution, which is consistent with the present observation illustrated in Fig. 5(a) and (b).

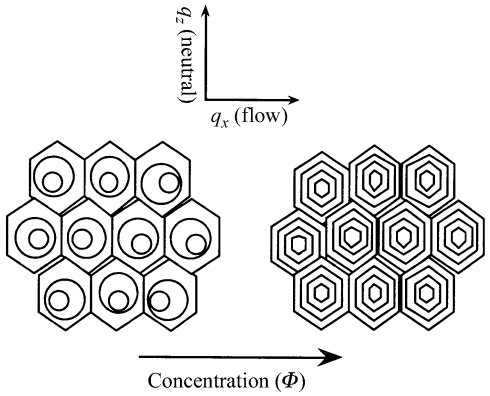

Fig. 6 Schematic representation of spherulites in dilute and concentrated samples. The anisotropy (hexagonal structure) in the 2-D SANS spectra is caused by the interactions between the closely packed MLVs propagating far into the inner layers, which is more prevalent at $\Phi = 0.44$ (right) than at $\Phi = 0.2$ (left).

Fig. 7 shows mesh plots of hexagonal scattering spectra from the $\Phi = 0.44$ sample: (top) sheared at 100 s^{-1} and (bottom) at rest, 360 s after cessation of shear. At rest, all the six spots have the same intensity and the same absolute q-value. When the sample is sheared, however, we observed variations in the intensity. These intensity variations indicate a slight tilt of the bilayer normals with respect to the flow–neutral (q_x, q_z) plane. The q-vector of the experiment does not lie completely in the flow–neutral plane, but makes an angle with respect to this plane of $\theta/2$, where θ is the scattering angle. If we consider, for example, the two Bragg peaks along the horizontal direction where $q_z = 0$, the intensity difference indicates that the normal of the bilayer stacks that give rise to these peaks is slightly tilted away from the flow direction. In this way, the layer normal makes a smaller angle with the

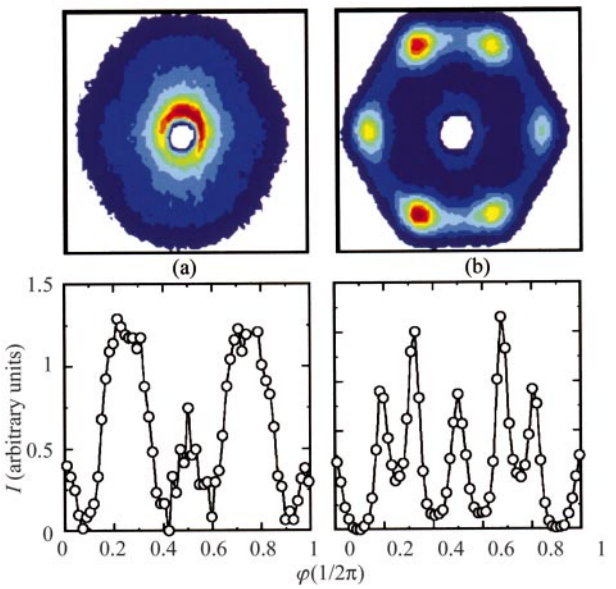

Fig. 5 Hexagonally packed multilamellar vesicles (spherulites). The two examples shown are from (a) $\Phi = 0.23$ and (b) 0.44 samples measured at 42.0 and 38.7 °C, respectively. For illustration purposes, the scattering intensity in (a, bottom) was multiplied by a constant (16.6).

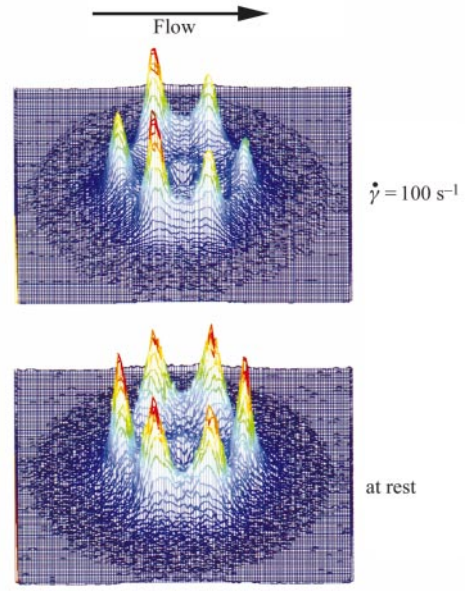

Fig. 7 3-D mesh plots of SANS measurements obtained for a $\Phi = 0.44$ sample in state **ii**. The data shown are from a heating experiment shearing at a rate of 100 s^{-1} (top) and after cessation of shear for 360 s (bottom). The temperature was kept constant at 39.3 ± 0.1 °C.

q-vector on one side compared to the other, thus giving different intensities at the two different q-vectors. This tilting is expected if the MLVs are organized into layers of constant velocity stacked in the gradient direction. This implies that flow is maintained by having the layers of different velocities sliding on top of each other. Such layering and layer sliding have, for example, been observed in sheared colloidal suspensions[21,22] and were also proposed to occur in another MLV system.[11] The velocity of the layers decreases when going from the inner to the outer cylinder, thus a given layer is sandwiched between two other layers having different relative velocities. The resulting shear stress makes an elastic deformation of the layer that tilts the bilayer stacks. When the shear is turned off, the shear stress relaxes as the bilayer stacks relax to the symmetrical hexagonal structure. The proposed MLV organization is schematically illustrated in Fig. 8.[23] Note that under shear the six spots do not have exactly the same absolute q-value, *i.e.* there is a slight deviation from hexagonal symmetry. This variation indicates a minor elongation of the MLVs, and thus a larger bilayer spacing, in the flow direction.

We can rationalize the packing in state **ii** as follows: The volume fraction of an MLV is defined as:

$$\Phi_{\mathrm{MLV}} = \frac{V_{\mathrm{MLV}}}{V_{\mathrm{tot}}} = \frac{N[4\pi(n_{\mathrm{sh}}\, d_{\mathrm{MLV}})^3]/3}{V_{\mathrm{tot}}}, \tag{10}$$

where N is the number of vesicles, and the bilayer area stored in an MLV structure is

$$A_{\mathrm{MLV}} = 4\pi d_{\mathrm{MLV}}^2 \frac{n^3}{3}. \tag{11}$$

For nonionic systems, the interfacial area is conserved, *i.e.* $A_{\mathrm{tot}} = NA_{\mathrm{MLV}}$, and we obtain the following relation

$$\frac{NA_{\mathrm{MLV}}}{V_{\mathrm{tot}}} = \frac{\Phi}{l_{\mathrm{b}}} = \frac{1}{d_{\mathrm{L}_\alpha}}. \tag{12}$$

where l_{b} is the effective or dry bilayer thickness. A value of $l_{\mathrm{b}} = 29$ Å was obtained from a plot of d_{L_α} *vs.* Φ^{-1} and agrees well with X-ray measurements on the same system.[24] Substituting eqns. (11) and (12) into eqn. (10) we arrive at:

$$\Phi_{\mathrm{MLV}} = \frac{d_{\mathrm{MLV}}}{d_{\mathrm{L}_\alpha}}. \tag{13}$$

Experimentally one often finds $d_{\mathrm{MLV}} \approx d_{\mathrm{L}_\alpha}$ which essentially means that the packing of MLVs is very dense, as also suggested by the rheological properties. The high packing density in most systems is realized by a polydisperse arrangement of large and small MLVs, where the smaller ones occupy the voids between the larger MLVs. However, if the polydispersity decreases, keeping $d_{\mathrm{MLV}} \approx d_{\mathrm{L}_\alpha}$ means that the MLVs have to depart from the spherical shape and pack into honeycomb arrangements. The latter agrees well with the observed scattering pattern and the layering scenario.

The fact that $d_{\mathrm{MLV}} \approx d_{\mathrm{L}_\alpha}$ is interesting is that the MLVs could expel solvent and thereby decrease their volume fraction. This is apparently prevented by a sufficiently low osmotic compressibility. Near close packing of the hydrated bilayers, the compressibility is low, but is expected to decrease significantly with dilution, and for lower concentrations we expect $d_{\mathrm{MLV}} < d_{\mathrm{L}_\alpha}$ leading to a less dense packing.

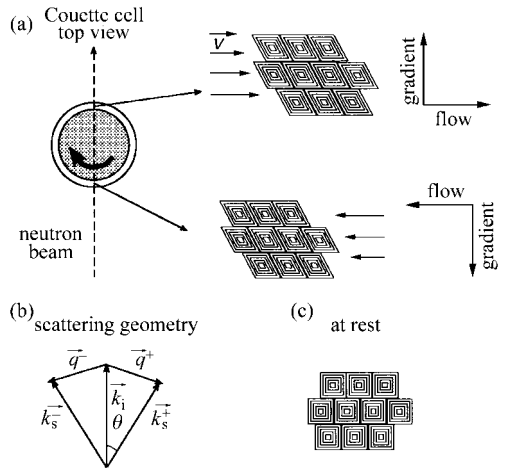

Fig. 8 Schematic illustration of the elasticity of spherulite deformation under shear. (a) Top view of the Couette cell. The spherulites are assumed to organize into uncorrelated layers, stacked in the gradient direction, and flow is maintained by the layers sliding against each other. The velocity gradient is given by the fixed shear rate. The shear stress deforms the spherulites causing them to become skew in the flow–gradient plane. The bilayer stacked in the flow direction will have their normal direction more parallel to $\vec{q}^-$ than to $\vec{q}^+$, resulting in a larger scattering intensity at $\vec{q}$ Scattering geometry: $\vec{k}_i$ is the wave vector of the incident beam, $\vec{k}_s^-$ and $\vec{q}_s^+$ are the wave vectors of the scattered beam, to the left and right, respectively. $\vec{q}^-$ and $\vec{q}^+$ are the resulting scattering vectors to the left and right, respectively, and q is the scattering angle. Note that the $\vec{q}^-$ and $\vec{q}^+$ are not completely parallel to the flow direction.

Conclusions

Temperature scan experiments under shear have been performed on a two-component ($C_{12}E_4$–D_2O) system using a small-angle neutron scattering (SANS) spectrometer. In the experiments, we fixed the shear rate at 100 s^{-1} and recorded 2-D SANS spectra while increasing (or decreasing) the temperature of the sample at a steady rate. The temperature dependent structural change is reversible and appears to be a general feature of nonionic surfactant systems of the type C_nE_m, *cf.* ref. 6. The present system under steady shear produces multilamellar vesicles (MLVs) at lower temperatures and transforms into a planar lamellar state at higher temperatures. The T-dependence can qualitatively be rationalized in terms of the temperature dependence of the monolayer spontaneous curvature, which decreases with increasing temperature. Particularly interesting is the observation of a state of closely packed honeycomb shaped MLVs within a certain temperature interval. Similar ordering has been found previously in ionic systems containing sodium dodecylsulfate, alcohol, and water.[11,25] This structure is formed as the MLV size distribution becomes narrow and the interlamellar spacing is conserved. The reason why in this system it only forms in a certain temperature interval is at present not understood.

Acknowledgements

This research was supported by the Swedish Natural Science Research Council (NFR). The neutron scattering experiments at Risø was supported by the EU-TMR program for Large Scale Facilities.

References

1 J. Arrault, C. Grand, W. C. K. Poon and M. E. Cates, *Europhys. Lett.*, 1997, **38**, 625.
2 A. Bernheim-Grosswasser, S. Ugazio, F. Gauffre, O. Viratelle, P. Mahy and D. Roux, *J. Chem. Phys.*, 2000, **112**, 3424.
3 F. Gauffre and D. Roux, *Langmuir*, 1999, **15**, 3738.
4 F. Gauffre and D. Roux, *Langmuir*, 1999, **15**, 3070.
5 O. Diat, D. Roux and F. Nallet, *J. Phys. II* (*France*), 1993, **3**, 1427.
6 T. D. Le, U. Olsson, K. Mortensen, J. Zipfel and W. Richtering, *Langmuir*, in press.
7 O. Diat and D. Roux, *J. Phys. II* (*France*), 1993, **3**, 9.
8 H. Wennerström and D. M. Anderson, *Difference vs. Gaussian Curvature Energies*, Institute for Mathematics and Its Applications, Minneapolis, MN, 1991.
9 D. J. Mitchell, G. J. T. Tiddy, L. Waring, T. Bostock and M. P. McDonald, *J. Chem. Soc., Faraday Trans. 1*, 1983, **79**, 975.

10 M. Jonströmer and R. Strey, *J. Phys. Chem.*, 1992, **96**, 5993.
11 O. Diat, D. Roux and F. Nallet, *Phys. Rev. E*, 1995, **51**, 3296.
12 S. Müller, C. Börschig, W. Gronshi and C. Schmidt, *Langmuir*, 1999, **15**, 7558.
13 C. W. Macosko, *Rheology: Principles, Measurements and Applications*, VCH Publications, Inc., New York, 1994.
14 K. Mortensen, K. Almdal, F. S. Bates, K. Koppi, M. Tirrell and B. Nordén, *Physica B*, 1995, **213–214**, 682.
15 The slight anisotropy in the scattering data from states **i** and **iii** indicates a minor departure from the spherical MLV shape. The contrast relative to state **ii** is, however, significant.
16 J. Bergenholtz and N. J. Wagner, *Langmuir*, 1996, **12**, 3122.
17 E. van der Linden and W. T. Hogervorst, *Langmuir*, 1996, **12**, 3127.
18 P. Panizza, A. Colin, C. Coulon and D. Roux, *Eur. Phys. J. B*, 1998, **4**, 65.
19 T. D. Le, U. Olsson, H. Wennerström and P. Schurtenberger, *Phys. Rev. E*, 1999, **60**, 4300.
20 B. Halle and P.-O. Quist, *J. Phys. II* (*France*), 1994, **4**, 1823.
21 M. Tomita and T. G. M. van de Ven, *J. Colloid Interface Sci.*, 1984, **99**, 374.
22 B. J. Ackerson and P. N. Pusey, *Phys. Rev. Lett.*, 1988, **61**, 1033.
23 Fig. 8 shows the top view (looking down in the neutral direction) onto the flow–gradient plane. In this plane, we represent the MLVs as squares to focus on the bilayer part that has the normal (almost) parallel to the flow direction. Note that the structure in the gradient direction is not probed by the neutron beam. In Fig. 6, however, the flow–neutral plane is probed by the neutron beam.
24 H. Kunieda, K. Nakamura, H. T. Davis and D. F. Evans, *Langmuir*, 1991, **7**, 1915.
25 P. Sierro and D. Roux, *Phys. Rev. Lett.*, 1997, **78**, 1496.